MATEC Web of Conferences **207**, 04003 (2018) https://doi.org/10.1051/matecconf/201820704003
ICMMPM 2018

Laser Micromilling Technology as a Key for Rapid Prototyping SMD ceramic MEMS devices

Nikolay Samotaev[1,a], Konstantin Oblov[1] and Anastasia Ivanova[1]

[1]*National Research Nuclear University MEPhI (Moscow Engineering Physics Institute), 115409, Kasirskoe highway 31, Moscow, Russia*

Abstract. The flexible laser micromilling technology for ceramic MEMS producing of microhotplate in the surface mounted device (SMD) package for the metal oxide (MOX) gas sensors is describing. There are discusses technological and economic aspects of small-scale production of gas MOX sensors in comparison with classical clean room technologies using for mass production MEMS devices. The main technical factors affecting on using MOX sensors in various applications are presented. Current results demonstrate that using described technology possible to manufacturing all parts of MOX gas sensor in the SMD form-factor SOT-23 package type.

1 Introduction

The modern MOX sensor is a combination of several factors – a microhotplate (responsible for power consumption and temperature operation mode), MOX gas sensitive layer (responsible for sensitivity to target gases) and a package (responsible for the possible applications of MOX gas sensor) [1]. Last decades MOX gas sensors development there is a concentration of efforts, in the field of technologies allowing obtaining a cheap product for mass applications in the manner of indoor air quality (IAQ) monitoring. Similar solutions were found by the leading manufacturers of MOX sensors (Figaro, Sensirion, Bosch, AMS, SGX, etc.) [2-6]. Technological solutions that make it possible to obtain a sensor with satisfactory characteristics for such application consist in the use of a combination of silicon MEMS microhotplate [2-6] and plastic [2,3], metal-plastic [4] or metal-ceramic [5, 6] SMD package. But what need to do scientific groups which, at the moment there is no market or market still small for the return of investment in silicon MEMS technology and the production of specialized plastic or ceramic SMD package? In that case need using technology process close to 3D prototype philosophy – rapid, simple and cheap with ratio a single sample to total production cost.

After several experiments with wide spectres ceramics MEMS technologies and materials (ZrO_2 [7], Al_2O_3 [8], LTCC ceramics [9]) we find more flexible technology responsible to goals of 3D prototype philosophy. As a technology for manufacturing ceramic MEMS MOX sensor and SMD package for one, we propose to use combination of laser micromilling monolithic Al_2O_3 commercially available ceramics and screen-print/jet (aerosol) printing technologies to form platinum metallization on MEMS and package.

2 Experiment

The equipment involved in the described laser micromilling technology does not need clean rooms and is widely presented on the market. The software for technology is simple and accessible at the student level (3D printing software with open access). The only specialized product of the proposed technology is software for adaptation of machine vision to obtain the minimum possible size of the MEMS structure of the microheater and the deposition of the MOX gas sensitive layer and platinum metallization, as well as the translation program of the MEMS 3D models of 2D topology of metallization to a 4-axis laser micromilling facilities for automatic production (Photo of tech process present on fig.1).

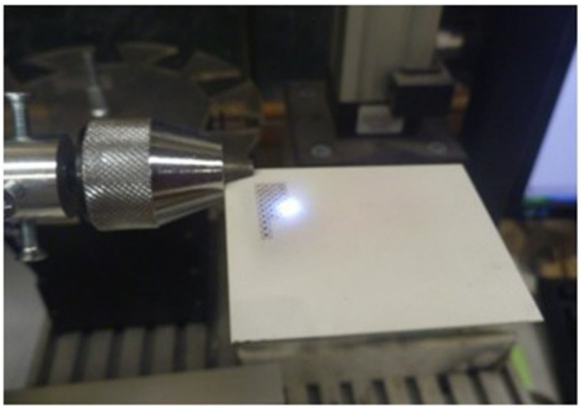

Figure 1. Photos of micromilling by 4-axis CNC 1,064 µm wavelength fiber laser tool 250 µm thick Al_2O_3 substrate during fabrication microhotplates for MOX gas sensor present on fig. 4 and 5.

[a] Corresponding author: nnsamotaev@mephi.ru

Technological steps for our experimental works are follows:
- 3D modeling of MEMS microhotplate, top and bottom part of the package (Fig. 2a, 2b) in *.stl format (Autodesk Inventor or SolidWorks program) and 2D modeling topology of MEMS metallization in *.dxf format (AutoCAD program),
- Simulation of the MEMS microhotplate parameters in the COMSOL program for prediction approximate representations about the MOX sensor thermal characteristics (optional),

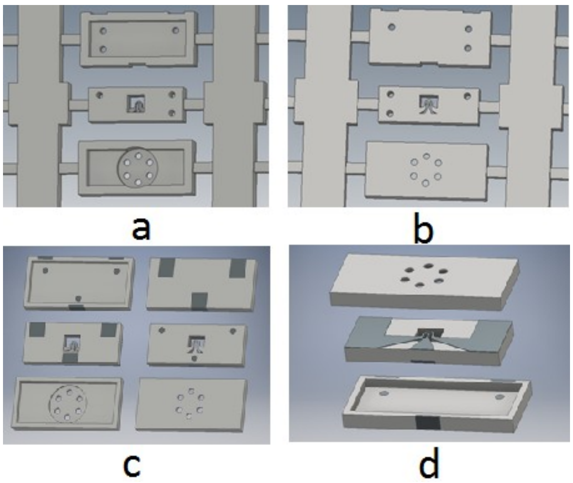

Figure 2. a) Bottom and b) Top view of 3D model of microhotplate and parts of SMD package as a task for laser micromilling. c) Scheme of metallization topology in 3D model. d) Scheme of assembling MEMS microhotplate in SMD package.

- Laser micromilling of monolithic ceramics on a 4-axis laser facility (Fig.1) by using 3D model of MEMS microhotplate, top and bottom part of the package (Fig 3),
- Deposition of platinum metallization using 2D model topology and technical annealing of metallization on MEMS according to specification on screen-print, jet or aerosol platinum materials (Fig. 2c),

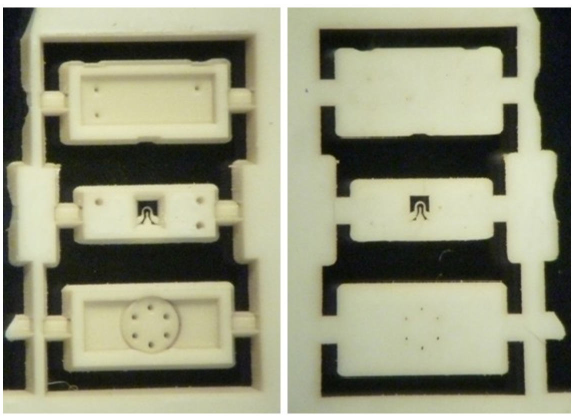

Figure 3. Photos of bottom (left) and top (right) views on 250 μm thick Al_2O_3 substrate with part of SOT-23 SMD package and microhotplate for MOX gas sensor after laser micromilling.

- Laser micromilling of metallization according 2D model (optional),
- Deposition and annealing of the MOX gas sensitive layer on the MEMS microhotplate,
- Assembling and conglutination by special glass single parts of sensor into a monolith package, like schematically represented for SOT-23 package on Fig. 2d.

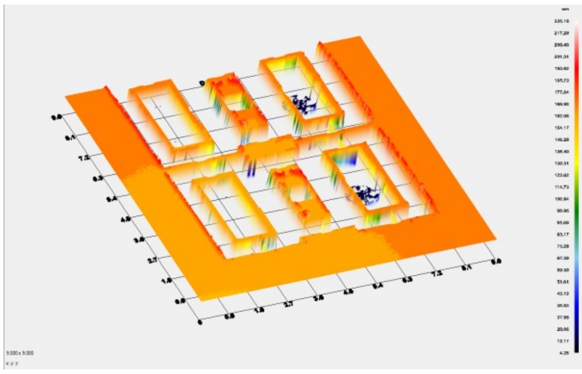

Figure 4. Dimensions parts of SMD package measured by optic noncontact profilometer. Standard SOT-23 packages dimension is 1,6 x 2,8 x1,0 mm.

Using present approach, experiments were carried out to fabricate a MEMS microhotplate, whose track width was 30 μm and a thickness of 20 μm (see Fig. 5). The power consumption of MEMS microhotplate at 450°C was approximately 250 mW (350 mW at ≈ 600°C – “burning” platinum temperature, see Fig. 6). Current results gives the prospect that manufacture MOX sensor in the SMD SOT-23 package type (max dissipating power by form-factor of package is 350 mW [10]) for surface mounting in a tape is available by using described technology.

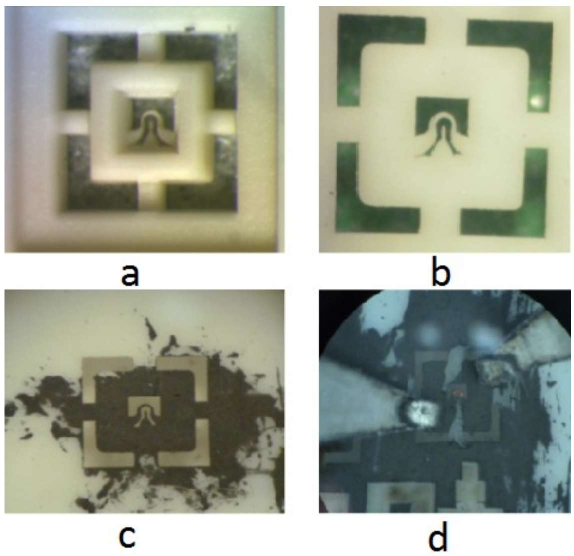

Figure 5. a) Bottom view of MEMS microhotpale after laser micromilling. Chip size 1,0 x 1,0 mm by border of internal frame. b) Top view of MEMS. Internal window size 0,3 x 0,3 mm. Central track width is 30 μm. c) Microheater track width 30 micron under cower Pt paste. d) Testing MEMS microhotplate under voltage load (pins). Hot area is ≈ 600°C.

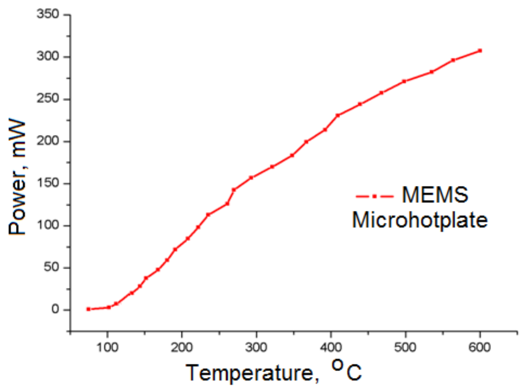

Figure 6. Power consumption of microhotplate fabricated by laser micromilling technology. Topology and SEM photo of MEMS microhotplate presents respectively on Fig. 7 and 8.

3 Discussion

Current experimental results gives prospects that manufacture MOX gas sensor in the SMD SOT-23 package type (max dissipating power by form-factor of package is 350 mW [10]) for surface mounting in a tape is available by using described above technology.

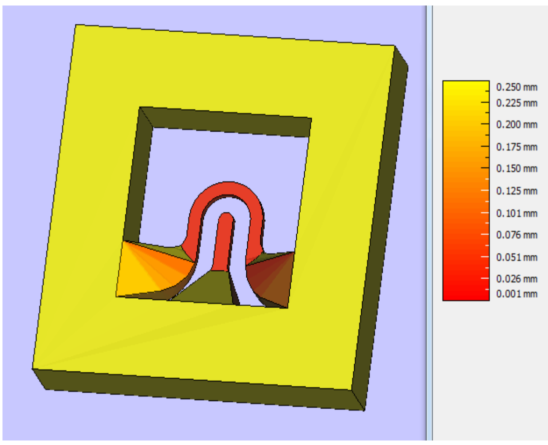

Figure 7. 3D model of MEMS microhotplate in *.stl format (Print Screen in Autodesk Inventor CAD program).

To control the accuracy of MEMS manufacturing, a scanning electron microscope was applied. On Fig.7 present 3D model of MEMS microhotplate as a print screen in Autodesk Inventor CAD program and for comparisons on Fig.8 present photo of the same MEMS microhotplate immediately after laser micromilling. From Fig.8 ensue that laser micromilling gives geometric dimensions withstand relatively well, opposite the roughness is the parameter on which depend from thickness.

The quality of the final MEMS structure strongly depends on its surface roughness. The minimal roughness will make the MEMS structure more durable, as well as allow for more qualitative metallization deposition processes on the chip surface. To obtain a minimum surface roughness, it is required to use a material whose thickness does not exceed the height of the obtained structure in order to avoid ablation of the volume of the material only in order to reduce its thickness. However, the cost of the final product depends heavily on the cost of the material, in our case, ceramic substrates Al_2O_3. The minimum cost have substrates with standard size. The standard sizes of the ceramic substrates being manufactured start at a thickness of 500 µm or higher, which, at a chip height of 250 µm, requires excess ablation of the material at a thickness of 250 µm. Operation of laser evaporation of excess material can be justified in the case of a high cost of manufacturing substrates of non-standard thickness and only in the case of a qualitatively selected laser micro-milling mode that does not lead to a strong increase in the surface roughness after removal of excess material thickness.

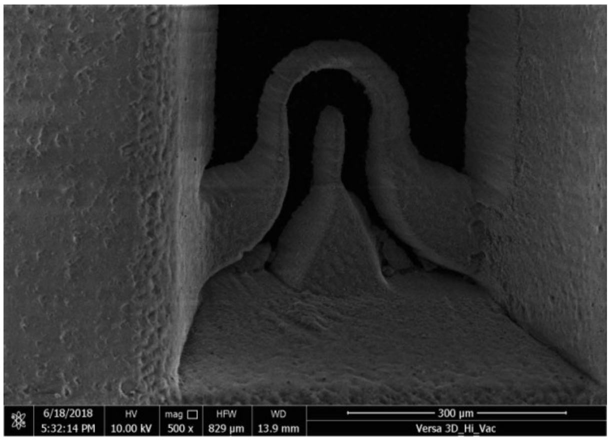

Figure 8. SEM photo MEMS microhotplate immediately after laser micromilling of 250 µm thick Al_2O_3 substrate using 3D model of MEMS microheater in *.stl format as a source CNC-code.

Laser radiation allows carrying out the process of Al_2O_3 ceramics ablation to a depth of 0.5 to 10µ in one pass. High radiation power and low speed of the laser beam accelerate the process of micro-milling, but lead to a higher surface roughness, the values of which can be more than 50 µm. Roughness is formed due to the fact that the intensity of laser radiation has a Gaussian distribution, which requires a very accurate selection of the laser beam overlapping region, when the entire material is engraved. On average, the surface roughness is 50 percent of the ablation depth per one pass of the laser beam. The minimum roughness was obtained by evaporation of the material in one pass at 1 µ and amounted to 2.3 µ.

The laser micro-milling process is a complex multifactor physical process, whose behaviour, depending on the type of material being processed, has a different character, which requires an empirical selection of the optimal surface treatment regime. Acceleration of the debugging process can be achieved by integrating the measuring equipment, able to produce a visual analysis of the surface obtained. After the ablation of each layer of material, such integration allows to analyze the resulting surface and correct the laser radiation regime by adjusting the radiation parameters or introducing additional cleaning passages aimed only at the surface roughness reducing. Suchlike machine learning is the task for specialized software developed within the framework of described technology.

Production time for laser micromilling of single MEMS structure was ~ 10 minutes, and 1 hour is necessary for group annealing of the MEMS metallization on substrate using muffle furnace. Our experience shows that, if technology is used by skilled personals, that gives fantastic design and manufacturing speed for ready-to-use microhotplates (about 2 hour)! The cost of materials (alumina substrate and platinum ink) for the manufacturing of single microhotplate with size of 1×1 mm is of about 0.50 Euro. The cost of a new set of equipment used in our experimental works is around 69k Euro.

4 Conclusion

We demonstrated that the application of laser micromilling technology for the fabrication of sensing MEMS devices is very prospective and assures important advantages in comparison with traditional expensive clean room technologies. These advantages are related first of all with a very considerable enlargement of the range of working temperatures (up to 800 ^{0}C) and of the range of technological treatment temperature of the sensor (up to almost 1000 ^{0}C compare with maximum 720 ^{0}C for silicon technology). This enlargement of temperature range results in the possibility to detect gases, not detectable with silicon based devices and to improve significantly the selectivity of gas sensors using temperature modulation regime of operation [10]. Another important result is the possibility to fabricate sensors operating under harsh environmental conditions including industrial and natural catastrophes using ceramic material stable for high temperatures and aggressive agents.

Acknowledgement

This work was supported by the Ministry Education and Science Russian Federation (Grant No. 14.584.21.0030 from 22.11.2017, unique identifier RFMEFI58417X0030) in frame of joint Russian-Korean project.

References

1. I. Simon, N. Bârsan, M. Bauer, U. Weimar, U. Sensors and Actuators, B, **73 (1)**, (2001).
2. https://www.sensirion.com/en/environmental-sensors/gas-sensors/
3. http://ams.com/eng/Products/Environmental-Sensors/Gas-Sensors/AS-MLV-P2
4. https://www.bosch-sensortec.com/bst/products/all_products/bme680
5. https://www.sgxsensortech.com/content/uploads/2014/08/1107_Datasheet-MiCS-2714.pdf
6. http://www.figarosensor.com/products/entry/tgs8100.html
7. A. Vasiliev, A. Lipilin, A. Mozalev, A.S. Lagutin, A. Pisliakov, N. Zaretskiy, N. Samotaev, A. Sokolov, Proc. of SPIE, **8066**, (2011).
8. A. Vasiliev, R. Pavelko, S. Gogish-Klushin, D. Kharitonov, O. Gogish-Klushina, A. Sokolov, A. Pisliakov, N. Samotaev, Sensors and Actuators, B, **132 (1)**, (2008).
9. A. Vasiliev, A. Pisliakov, A. Sokolov, N. Samotaev, S. Soloviev, K. Oblov, V. Guarnieri, L. Lorenzelli, J. Brunelli, A. Maglione, A. Lipilin, A Mozalev, A. Legin, Sensors and Actuators, B, **224**, (2016).
10. https://www.diodes.com/assets/Datasheets/ds18001.pdf
11. N. Samotaev, B. Podlepetsky, A. Vasiliev, A. Pisliakov, A. Sokolov, Automation and Remote Control, **74 (2)**, (2013).